•OH oxidation of methionine in the presence of discrete water molecules: DFT, QTAIM and valence bond analyses

Jacqueline Bergès, Dominik Domin, Julien Pilmé, Benoît Braïda, Chantal Houée-Levin

•OH Oxidation of Methionine in the presence of discrete water molecules. DFT, QTAIM and Valence Bond analyses

Jacqueline Bergès[1], Dominik Domin[2], Julien Pilmé[1], Benoît Braïda[1], and Chantal Houée-Levin[3]

[1] Sorbonne université, CNRS UMR 7616, Laboratoire de Chimie Théorique, Case Courrier 137, 4 Place Jussieu, 75252 Paris, France.
[2] Faculty of Biotechnology, Chemistry and Environmental Engineering, PHENIKAA University, Hanoi 12116, Vietnam
PHENIKAA Institute for Advanced Study (PIAS), PHENIKAA University, Hanoi 12116, Vietnam
Previous Affiliation : Direction de la Recherche Fondamentale, Maison de la Simulation, Bâtiment 565 –Digiteo, Commissariat a l'Energie Atomique, centre de Saclay, 91191 Gif-sur-Yvette Cedex.
[3] Laboratoire de Chimie Physique, Université Paris sud, Université Paris Saclay, CNRS UMR 8000, 91400 Orsay France

Corresponding authors
Jacqueline Bergès: jb@lct.jussieu.fr
Julien Pilmé: pilme@lct.jussieu.fr

ABSTRACT. The first steps of the oxidation process of amino acid methionine (Met, CAS 63-68-3) by •OH radicals, leading to Met-OH• adduct and then to Met radical cation, were investigated theoretically over the last few years considering the aqueous environment as a continuum. In this work, following the same procedure that we used for the oxidation of dimethyl sulfide (Domin et al. (2017) J Phys Chem B, 121:9321), discrete water molecules as well as relative positions of the OH radical to Met were taken from Molecular Dynamics calculations. The presence of water molecules strongly modifies the relative energies of Met-OH adducts and cations when water is properly modeled. Depending on the terminal functional groups and on the position of the •OH radical several stable structures were found, however the most stable radical is the N-centered or the S∴N radical cation. QTAIM analysis and Valence Bond (VB) treatment allowed for the characterization of the 2c∴3e nature of S∴N and S∴OH bonds. VB analysis estimated the probability of the heterolytic rupture of the OH adduct that is modified by the presence of water molecules.

Keywords. Oxidation of Methionine by OH radicals; explicit water molecules; DFT calculation; QTAIM; VB analysis; two center-three electron bonded radical.

Electronic supplementary material. This article contains supplementary material.

Introduction

Sulfur containing molecules are major targets of reactive oxygen species (ROS) in biological media. A wealth of experimental results has shown that •OH radicals oxidize quickly and efficiently these biomolecules. The oxidation of these compounds has numerous consequences *in vivo*. The primary mechanism begins by the formation of an >S-$^{\bullet}$OH adduct which would dissociate into a sulfur centered cation radical and a hydroxide molecule (Reactions (1) and (2)).

(1) $>S + {}^{\bullet}OH \rightarrow >S\text{-}{}^{\bullet}OH$

(2) $>S\text{-}{}^{\bullet}OH \rightarrow >S^{\bullet+} + OH^{-}$

The oxidation mechanism of the methionine (Met) amino acid or residue in peptides by $^{\bullet}$OH radicals has been largely studied experimentally from the very first steps (reaction (1)) [1-5] to the final compounds [6-8]. It is well known that Reaction (1) is dominantly diffusion-controlled for the amino acid as well as for Met residues in peptides and proteins [9] and that it is followed by several rearrangements triggered by Reaction (2). Due to the complexity of the following steps, this wealth of experimental data had to be completed by numerous computational works [5, 8, 10-17]. These studies were mainly focused on deciphering the nature of transient species, their stability and their eventual reactivity. Indeed, it has long been suggested [2] that the sulfur centered radical cation may undergo some kind of cyclization by forming a two-center three electron bond (2c-3e) with a heteroatom that has a lone pair (see [4-5] and references therein for reviews on the matter). Recent Density Functional Theory (DFT) calculations (using the BH&HLYP functional) and Quantum Chemical Topology analysis confirmed the stability of cyclic species containing 5 to 9 atoms in dipeptides [13-14]. The eventual reactivity of the methionine radical cations has also been studied in the view of predicting possible intra- or intermolecular electron transfers in proteins. It has been shown that the redox potential of methionine radicals in peptides varies with the nature of the vicinal residue, the geometry and the size of the pseudo cyclic group [11-12]. This finding provides the basis for understand, for instance, why in some cases long range intramolecular electron transfer occurs from tyrosine to the methionine cation radical. In Met enkephalin, the electron transfer pathway has been computed [18]. Finally, many authors have considered the oxidation reaction in the presence of oxygen [19].

In these simulations, the main difficulty is with the description of the solvent and in the choice of the terminal functional groups of the amino acid in order to provide a more realistic view of protein oxidation and avoiding charge. The solvent was frequently modeled by a continuum (CPCM or IEFPCM [13, 19], or by a dielectric constant [20]).This crude description lacks explicit molecular solvation layers that may participate in the oxidation mechanisms. Chu and co-workers added some explicit water molecules in the study of a related reaction, the oxidation of dimethylsulfide (DMS) and Met by H_2O_2 [21].

Moreover, for only Met embedded in a continuum, several terminal functional groups were tested : the simple zwitterion [22] $-CO_2CH_3$ and $-NH_3^+$ end groups, neutral Met with $-CO_2H$ and $-NH_2$ terminal functional groups in the gas phase [19], two peptide groups $-CO_2NH_2$ and $-NH_2CO_2$ [20].

In this work, we reinvestigated the electronic factors controlling both reactions (1) and (2) for the oxidation of methionine by $^{\bullet}OH$ radicals. We focused on the role of solvation layer by adding discrete water molecules to a CPCM continuum description. In a recent study [23] some of us have simulated using Molecular Dynamics (MD) the positions of discrete water molecules and $^{\bullet}OH$ radicals surrounding the simplest organic sulfur compound: dimethyl sulfide DMS. Here we have used the same simulation methodology for the methionine amino acid. The positions of the water molecules as well as various conformations of Met and the position of •OH radicals were obtained from MD simulations. Like in the previous study of the oxidation of DMS, waters within a radius of 4 Å around methionine were selected from several randomly selected snapshots of an equilibrated MD simulations. The $^{\bullet}OH$ radical could be close to O and N atoms in different conformations of Met. We especially focused on two initial types of conformations: folded with the sulfur atom close to the nitrogen atom (in the MetSN species) or to one of the oxygen atoms (in the MetSO species). Thus, we explored the stabilities of the folded conformations of various Met derived $^{\bullet}OH$ adducts (MetSN-OH and MetSO-OH).

Methionine was methylated to avoid the influence of the terminal groups in the zwitterions (electrostatic interactions between $-NH_3^+/-CO_2^-$ and the water molecules) i.e. the end groups were $-CO_2CH_3$ and $-NH_2CH_3$. To test the importance of the terminal functional groups, we replaced the amine methyl group by the amide group (mimicking a peptide bond) in some calculations.

Whenever possible we described the cations resulting from OH^- elimination with the same computational methodology and we drew the energetic landscape of their various conformations. Since the nature of bonding in the different compounds is of interest, a Valence Bond (VB) type of analysis can be revealing (for review see [24] and references within). Previous VB calculations have indeed shown that the interaction between a $^{\bullet}OH$ radical and one of the sulfur lone pair electrons of a methionine derivatives, may lead to either a weak electrostatic adduct, or to a stronger two-center three-electron bond, depending on the chemical groups linked to the sulfur [14, 23].

Computational methods

In the first step, MD simulation with geometries of the solute molecules kept fixed, were performed in an environment containing a very large number of explicit water molecules, i.e. more than 2000 water molecules in each periodic boundary condition unit cell. The CHARMM CGenFF 3.0.1 force field was used for these solute molecules and the CHARMM modified rigid TIP3P water model [25-27] was used for the solvent. The molecules were solvated by water in 20 Å in each direction. For the charged species, the force field parameters were obtained for the analogous neutral methionine and the net formal charge was placed on the sulfur atom. Subsequently from these equilibrated MD trajectories randomly selected snapshots where used for extracting nanodroplets containing ~70 solvent water molecules for further geometry reoptimization using the BH&HLYP functional, 6-31+G** basis set and a PCM explicit solvation model to account for the rest of the bulk water. From the latter optimized microsolvated structures, only the few water molecules in the first solvation shell that were directly in interaction with the Met-OH adduct were retained and used in subsequent highest level quantum chemistry calculations. Further geometry optimizations were carried out with BH&HLYP/6-311+g(d,p) on the clusters of the solutes surrounded by explicit water molecules selected in the previous MD steps. Note that it was previously shown [14] that optimizations using the DFT functional BH&HLYP, seemed specially adapted to describing radicals that contain 2c-3e bonds. The clusters were embedded in an implicit solvent (CPCM) that modeled the bulk aqueous environment. All the purely QM (DFT) calculations were carried out using the Gaussian 09 suite of programs [28].

Quantum Theory of Atoms-In-Molecules (QTAIM). The aim of this approach is to answer questions about the chemical bonding in molecules and solids, and predict chemical reactivity trends. The methodology relies on the theory of gradient dynamical systems that

enables a partitioning of the 3D molecular space into topological basins via the properties of the gradient vector field of the total electron density [29]. As its use has been widely reviewed, the formalism is only briefly recalled here. The QTAIM atoms can be defined as the union of a nucleus with its associated electron density basin. The basins are delimited by zero-flux surfaces and the integration of the electron density over each basin directly provides its corresponding population. The QTAIM atomic charge, q(A), is calculated by subtracting the electron population of the topological atom A from its atomic number. The atomic spin density is calculated as the difference between the both alpha and beta populations. Introduced by Bader and Stephens [30], and later recovered by Fradera et al. [31], the QTAIM delocalization index (DI) is a measure of the electron-sharing between two atoms and can be sometimes compared to other bond order indices.

Valence Bond Analysis. In a previous article [23], three of us have shown that, in the specific case of a (2c-3e) bond, the weights of the VB structures could be faithfully estimated from a spin density analysis obtained after a correlated MO-based calculation. The equations derived can be easily generalized in the present case by equations 1-3, where ω_i are the estimated weight of structure i, and ρ_A the spin density value on atom A. A proper description of a (2c-3e) bond has been shown to be potentially problematic both for DFT [32] and post-HF calculations [33,34]. However, levels of calculation such as BH&HLYP functional, or the Coupled-Cluster CCSD method, can typically provide estimated ω_i that have been shown to be in good agreement with those computed using the high level BOVB Valence Bond method.

$$\begin{cases} \omega_1 = \dfrac{\rho_O}{\rho_O + \rho_S + \rho_N} & (1) \\ \omega_2 = \dfrac{\rho_S}{\rho_O + \rho_S + \rho_N} & (2) \\ \omega_3 = \dfrac{\rho_N}{\rho_O + \rho_S + \rho_N} & (3) \end{cases}$$

Results and discussion on the adducts Met-OH

We focused on two aspects of the complexes: the position of the •OH radical relative to the molecule and the proximity of the sulfur atom to either nitrogen or to one of the oxygen atoms (MetSN or MetSO respectively). We selected four types of initial complexes coming directly from MD snapshots. These complexes are depicted on Scheme 1 where the •OH locations close to atoms S, N or O of Met have been surrounded by circles. The optimized geometries of these complexes, surrounded by a continuum CPCM, are depicted on Figure 1. In the complexes **MetSN-OH** (***I***) and **MetSO-OH** (***IV***), the S-OH bond is typically close to

2.3-2.4 Å. In contrast, the complex **II (*II*)**, •OH radical is close to both S and N atoms. The spin densities are found to be fairly distributed between S and N, with a S-N distance of 2.5 Å. In the complex **III (*III*),** the •OH radical is close to nitrogen only when S-N distances are short. Another complex was found with short S-N and S-•OH distances (2.4 Å) (not displayed on Figure 1). This complex was found instable and after the optimization process, the calculation led back to ***I.***

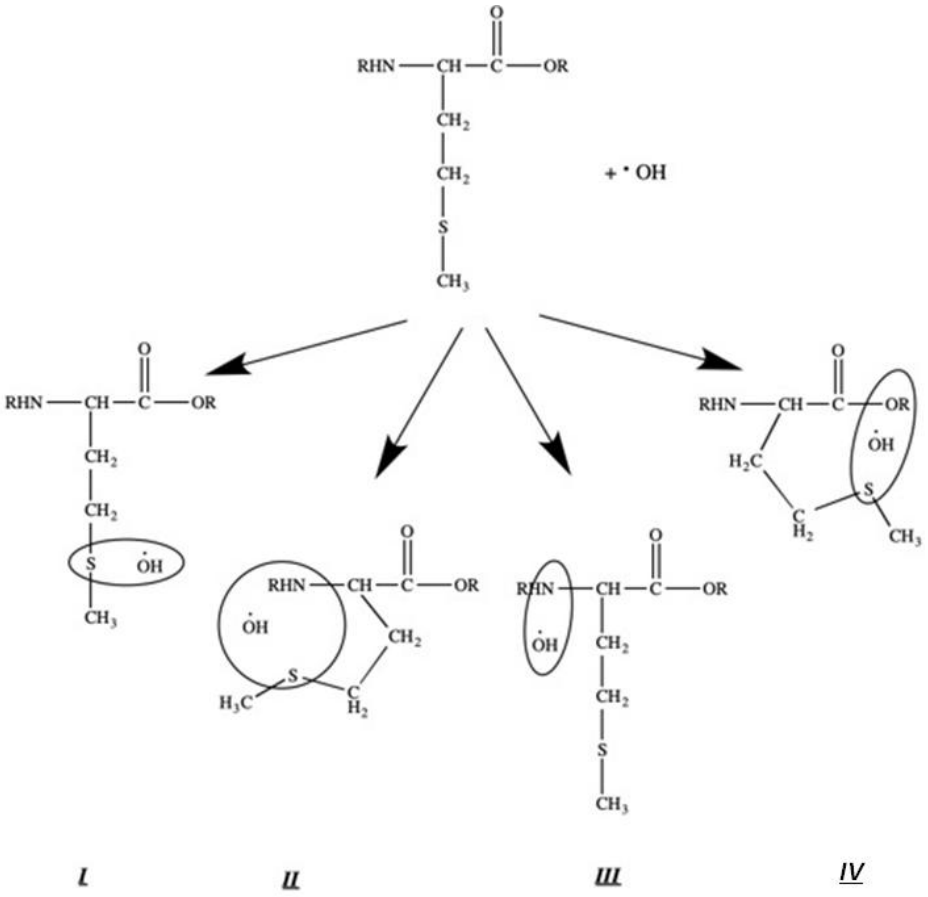

Scheme 1. Schematic complexes of MetSX-OH (x = NH, O) extracted from the MD snapshots. Circles identify the location of the •OH radical close to atoms S, N or O of Met.

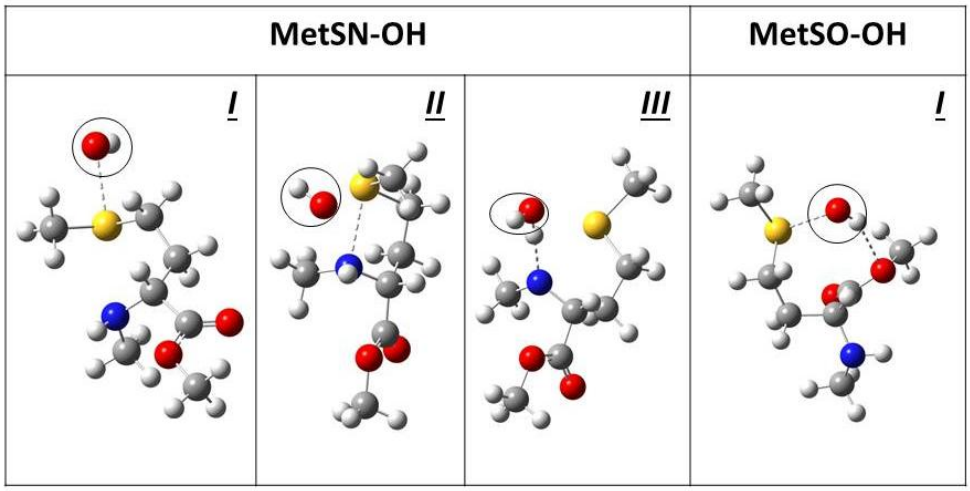

Figure 1. Conformations of MetSX-OH (x = NH, O) extracted from the MD snapshots and optimized at the BH&HLYP/6-311+g(d,p) + CPCM level of theory.
For all these conformations the bonds of 2.4 Å are represented by dotted lines.
Circles identify the location of the •OH radical.

Comparison of continuum model vs. QM/MM. First of all, we have tested the accuracy of the continuum model by comparison with QM/MM calculations, as we did for DMS [23], Met being a longer and more flexible molecule than DMS. The optimized geometries of two structures of ***I*** and ***IV*** were performed. In the QM/MM methodology, the positions and energies of 40 water molecules, initially found by MD in a 4 Å sphere, were calculated by the classical potential UFF/Qeq. (Table S1, column 1). In the alternative methodology, the solvent was described by a continuum modeled by CPCM (Table S1, column 2 & 3).

As observed in Table S1, both methods led to similar bond lengths and spin density distributions. In addition, the adducts MetSN-•OH and MetSO-•OH had very close electronic energies ($\Delta E \approx 2$kJ/mol, Table S1). In both cases ***I*** and ***IV***, spin densities and atomic charges were compared with three different schemes: Mulliken, QTAIM and NBO analysis. The three different models of atomic charges and spin densities led to similar conclusions. S and •OH always shared the spin densities, i.e. were linked by 2c-3e bond as observed for DMS-OH [23]. No S∴N or S∴O bond was formed. The partial charges remain mainly distributed on both the $S^{(\delta+)}$ atom and $OH^{(\delta-)}$group. This is consistent with the spin density analysis and also with the delocalization index, which supports this statement since the sulfur interacts mainly with the oxygen atom of OH while the S-N interaction remains negligible. Thus, further

calculations were performed using CPCM continuum model and further bonding analyses were preformed with the QTAIM method.

Continuum CPCM model only. Starting from points selected from MD where various positions of •OH around Met have been found, fully optimized calculations were performed using the BHHLYP/6-311+g(d,p) + CPCM level of theory. Table 1 gives the energetic and structural parameters together with QTAIM analysis for the ***I***, ***II***, ***III*** and ***IV*** complexes.

	Met**SN**-OH			Met**SO**-OH
E +954	-0.76835	-0.73997	-0.80062	-0.76909
Complexes	***I***	***II***	***III***	***IV***
ΔE_1	84.6	158.1	0.0	82.7
ΔE_2	0.0	73.5		1.9
d_{S-X}	3.38	2.48	3.20	3.51
d_{S-OH}	2.34	3.10	4.20	2.39
d_{N-H}			1.86	
ρ_S ; ρ_{XH} ; ρ_{OH}	0.38 0.0 0.61	0.56 0.38 0.0	0.0 0.96 0.0	0.32 0.00 0.66
Q_S ; Q_{OH}	0.19 -0.63	0.30 -0.94	0.30 -0.94	0.14 -0.32
δ_{S-X} δ_{S-OH}	0.04 0.62	0.48 0.10	0.06 0.02	0.00 0.56

Table 1. MetSX-OH folded complexes (with X=NH for **MetSN-OH** or X= O for **MetSO-OH**) computed at the BHandHLYP/6-311+G(d,p) + CPCM level of theory. Electronic energies (E) are given in a.u.. ΔE_1 is the relative energy with respect to the structure ***III*** given in kJ/mol. ΔE_2 is the relative energy with respect to the structure ***I*** given in kJ/mol. Selected distances are given in Å. QTAIM Spin densities: ρ_S ; ρ_{XH} ; ρ_{OH} and charges: Q_S ; Q_{OH}. δ_{S-N} and δ_{S-OH} are the delocalization indexes of the S-X and S-OH bonds are given in a.u..

As observed in Table 1, the optimized complex ***I*** displays a small S-OH distance (2.34 Å) and spin densities are distributed between S and OH (ρ_S = 0.38 a.u. and ρ_{OH} = 0.61 a.u.). In the starting point of ***II***, the hydroxyl radical was close to S and to N with S-N and S-OH distances were relatively short. After optimization, the S∴N bond became shorter. The spin densities are fairly distributed between S and N (ρ_S = 0.56 a.u. and ρ_{NH} = 0.38 a.u.)**.** With regards to the delocalization index δ_{S-N}, it remains lower than 0.5. These results are in good agreement with a 2c-3e bonding scheme for the S-N bond. Complex ***II*** is less stable than ***I*** by ≈ 80 kJ/mol. Conversely, the S-N distance was initially short in ***III***, while S and OH were far from each other. The optimized complex ***III*** corresponds to a hydrogen transfer that took place from the amino group to the •OH radical formation of a water molecule (see Figure 1), the spin density being mainly localized on the N center (ρ_{NH} = 0.96 a.u)**.** For the optimized complex ***IV***, OH radical is close to both S and one of the oxygen atoms (2.39 Å) and the spin densities are found distributed between S and OH (ρ_S = 0.32 a.u. and ρ_{OH} = 0.66 a.u)**.**

MetSN-•OH	***III init***	***III***	***III amide***
E + 954	-0.73388	-0.80062	E = -1068.106410
d_{S-N}	2.52	3.20	2.56
d_{S-OH}	5.96	4.20	2.86
d_{N-OH}	3.44	1.86	4.12
ρ_S ; ρ_{NH}	0.52 0.41	0.0 0.96	0.36 0.52
Q_S ; Q_{OH}	0.24 -0.98	0.30 -0.94	0.15 -0.73
δ_{S-N} δ_{S-OH}	0.10 0.00	0.06 0.02	0.44 0.00

Table 2. MetSN-OH folded complexes ***III*** have been optimized at the BHandHLYP/6-311+G(d,p) + CPCM level of theory. Electronic energies are given in a.u. Selected distances are given in Å. QTAIM Spin densities ρ_S ; ρ_{NH} and charges Q_S ; Q_{OH} are given in a.u.. δ_{S-N} and δ_{S-OH} are the delocalization indexes of S-N and S-OH bonds given in a.u.. Columns 1 to 2: the end groups are methyls and column 3: the end group of N is the amide.

As observed in Tables 1 and 2, ***III*** displays a OH charge close to -1.0 e and a typical strong spin density close to 1.0 only located on the nitrogen center. These results are consistent with the formation of a single N-centered radical and a water molecule bonded to the N-center with a hydrogen bond (Figure 1). When the methyl group of the N-terminus was replaced by the amide group $NHCOCH_3$ the H transfer from -NH and formation of a water molecule was also observed but a conformational change led to MetS$\therefore N^+$ 2c-3e bond like in ***II*** (see Table 1)

Addition of four discrete water molecules to MetSX-$^\bullet$OH (X=N or O). We selected four water molecules directly linked to the atoms S, N, O of Met and to the oxygen of $^\bullet$OH radical from the first solvation shell of Met-$^\bullet$OH, following the procedure used for the DMS adduct [23]. Figure 2 displays ***I***, ***II***, ***III*** and ***IV*** complexes surrounded by the 4 water molecules and Table 3 gathers optimized energetic and structural parameters together with QTAIM analysis.

	MetSN + 4 H_2O			**MetSO + 4 H_2O**
Complexes	***I***	***II***	***III***	***IV***
E+1260	-0.48570	-0.48276	-0.52360	-0.49264
ΔE	99.4	107.1	0.0	81.2
d_{S-X} ; d_{S-OH}	3.18 2.31	2.49 4.14	3.23 3.62	3.39 2.33
ρ_S ; ρ_X ; ρ_{OH}	0.46 0.00 0.51	0.52 0.21 0.00	0.00 0.97 0.00	0.48 0.00 0.50
Q_S ; Q_{OH}	0.26 -0.54	0.23 -0.85	-0.04 -0.74	0.25 -0.44
δ_{S-X} δ_{S-OH}	0.08 0.64	0.50 0.00	0.06 0.04	0.04 0.62

Table 3. MetSX-OH folded complexes (with X = NH or O) + $4H_2O$ are optimized at the BHHYP/6-311+G(d,p) + CPCM level of theory. Electronic energies (E) are given in a.u.. ΔE is the relative energy with respect to the structure ***III*** given in kJ/mol. Selected distances are given in Å. QTAIM Spin densities ρ_S, ρ_X, ρ_{NH} and charges Q_S, Q_{OH}. Delocalization indexes δ_{S-X}, δ_{S-OH} of S-X and S-OH bonds are given in a.u..

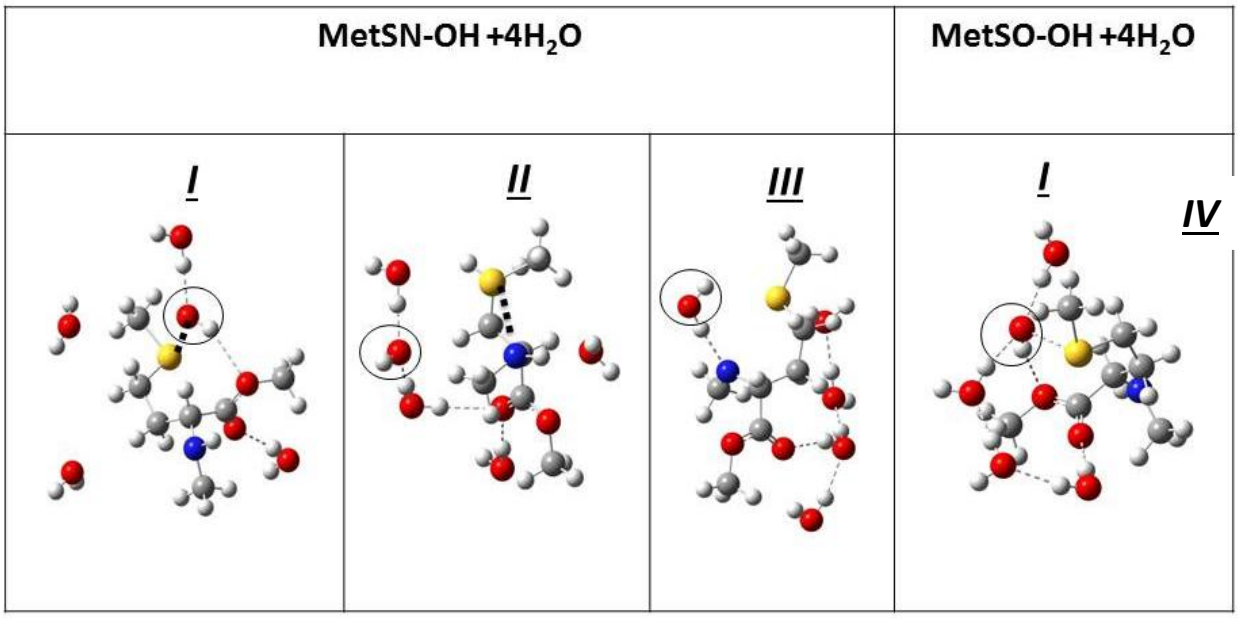

Figure 2. Stable conformations MetSX-•OH + 4H_2O.MetSN-OH (:***I***; ***II*** and ***III***)
Color code: gray dotted lines: hydrogen bonds, black: S-N and S-OH 2c 3e bonds.
Circles identify the location of the •OH radical.

In the presence of these discrete 4 water molecules, both ***I*** and ***II*** (Figure 2) have now rather close to relative energies (ΔE less than 8 kJ/mol) (Table 3), contrary to what was obtained when the aqueous environment was only modeled by CPCM (Table 1). The values of QTAIM descriptors (Table 3), are rather similar to those provided in Table 1 for all three complexes ***I***, ***II*** and ***III*** (**MetSN-OH + 4 H_2O)**.As for ***III*** + 4 H_2O (Figure 2), the result is also an H transfer from the amino group to •OH, leading to a N-centered radical and H_2O. Thus, the spin density ρ_{NH} reaches a strong value of 0.97, fully located on the N-center. Note that the charge Q(S) goes to almost zero (-0.04 e). The •OH radical was either interacting with the amino group or moved thanks to hydrogen bonds with another water molecule. This complex remains the most stable configuration and the relative energy has decreased because of the presence of water molecules (*ca.* 100 kJ/mol).

Three snapshots of the optimization process leading to ***III*** were extracted. Figure 3 displays the complexes of the initial point (obtained by MD) ***III*** and an intermediate point of the leading to optimized ***III*****.** The structural parameters and the QTAIM analysis are given in Table 4.

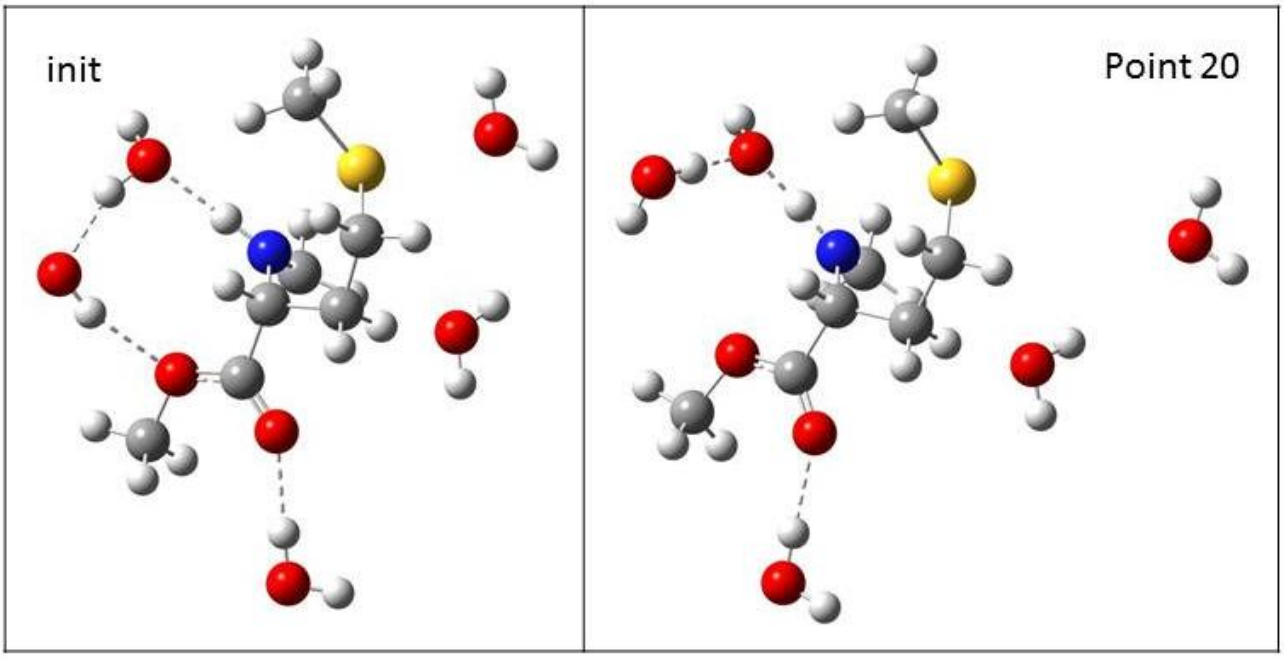

Figure 3. Conformations of the initial point (obtained by MD) and an intermediate point of the optimization leading to ***III*****.** Dotted lines: hydrogen bonds. Circles identify the location of the •OH radical.

MetSN+4 H_2O *III*	**First point**	**Intermediate point**	**(H-transfer)**
E + 1260	-0.43194	-0.47567	-0.51297
d_{S-N} d_{S-OH}	2.52 5.96	2.73 3.84	3.20 4.52
ρ_S ; ρ_{NH} ; ρ_{OH}	0.54 0.38 0.00	0.20 0.70 0.00	0.01 0.96 0.00
δ_{S-N} δ_{S-OH}	0.48 0.00	0.32 0.02	0.06 0.02

Table 4. Electronic (E) of ***III*** + $4H_2O$ structure along the H transfer has been computed at the BHHYP/6-311+G(d,p) + CPCM level of theory. Electronic energies (E) are given in a.u. Intramolecular distances S-N and S-OH are given in Å. QTAIM spin densities ρ_S ; ρ_{NH} ; ρ_{OH} and delocalization indexes δ_{S-N}, δ_{S-OH} of S-N and S-OH bonds are given in a.u..

During the H transfer process, the distances d_{S-N} logically increased from 2.52 Å to 3.20 Å whereas simultaneously, the d_{S-OH} decreased from 5.96 Å to 4.52 Å. Consequently, the delocalization index δ_{S-N} strongly decreased from 0.48 to 0.06. In addition, the spin density ρ_S fell to zero and ρ_{NH} reached a maximal value close to 1 at the end of the H-transfer process. This confirms that complex ***III*** exhibits a single radical center located on the nitrogen.

Actually, only ***II*** exhibits a SN 2c-3e bond. There is no 2c-3e SO bond. In the so-called MetSO-OH ***IV***, the most stable complex belongs to family ***I*** whatever the conformations of the carboxylate group (see Table S2): In $\boldsymbol{I_1}$ the sulfur is closer to the ester group while in $\boldsymbol{I_2}$, it is closer to the carbonyl group. Both exhibit common features with an electronic energy gap ΔE of less than 18 kJ/mol and a 2c-3e bond between S and $^{\bullet}$OH with distances of *ca*. 2.33Å (Table 3). These complexes are similar to the one obtained using only the CPCM model (Tables 1 and 2; Figures 1 and 2), the four water molecules forming a network of hydrogen bonds surrounding the adduct MetSO-OH.

To conclude, upon addition of four discrete water molecules the most important change is that now ***II*** has electronic energies close to that of ***I*** (ΔE 7 kJ/mol instead of 80 kJ/mol with CPCM only). The presence of 4 water molecules stabilizes the $MetSN^{\bullet+}$-OH cluster. Nevertheless, the most stable complex is still ***III,*** which undergoes H transfer from -NH to $^{\bullet}$OH leading to formation of a N-centered radical. Only two complexes of the adducts are likely to contribute to the heterolytic dissociation of the adduct leading to a radical cation $MetS^{\bullet+}$: ***II*** that could be considered as a precursor of $MetSN^{\bullet+}$ plus OH^{-} anion and ***I*** that, like in DMS-OH, can have a good probability to undergo this rupture depending on the chemical environment.

Valence Bond Analysis. The three-electron bond in the sulfur-OH case is characterized, within a VB formalism, by the resonance between VB structures 1 and 2 (see Scheme 2), with comparable weights for both structures. These two VB structures differ from a shift of one electron, and thus by a shift of charge, between the two bonded centers. Besides, the stability of the (2c,3e) bond arises from the resonance energy due to the mixing of the two structures, thus its classification as a "complete" charge-shift bond [24,25].

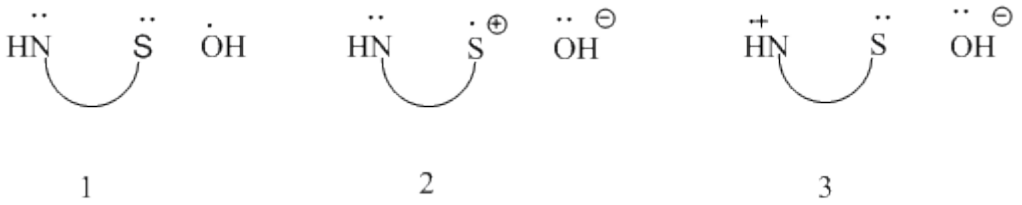

1 2 3

Scheme 2. Schematic representation of the three possible VB resonance conformations for the MetSN, MetSO and MetExt adducts with ˙OH.

A weak electrostatic adduct would correspond to the case where one of the two structures would be largely dominant in the description, and the other one negligible (~10% weight). In the case of the system studied here the situation is slightly more complicated, though. In conformations of Met where the nitrogen of the methionine is close enough either to the ˙OH radical or to the sulfur, it could also be involved in a (2c-3e) bond with either of the two. Therefore, a complete VB description involved the three VB structures displayed in scheme 2, where the radical could be delocalized on three different centers. Now five different cases could in principle occur: i) a weak electrostatic adduct, characterized by a largely dominant VB structure 1 and low weights for both VB structures 2 and 3; ii) a sulfur-oxygen (2c-3e) bond, with both VB structures 1 and 2 significantly resonance contributors while VB structure 3 has a negligible weight; iii) a nitrogen-oxygen (2c-3e) bond, characterized by a 1↔3 resonance and a low weight for structure 2; iv) a sulfur-nitrogen (2c-3e) bond, characterized by a 2↔3 resonance and a low weight for VB structure 1 ; v) when the three VB structures have comparable weights, which would correspond to a radical delocalized between the three atoms.

In Table 5, the estimated VB structure weights for ***I*** and ***II*** using the QTAIM spin densities, with or without explicit quantum description of the four water molecules corresponding to the first solvation shell, are displayed.

	ω_1	ω_2	ω_3
MetSN-OH *I* (-954.76835a.u.)	24	65	11
MetSN-OH + 4H_2O *I* (-1260.48570 a.u.)	45	54	1
MetSN-OH *II* (-954.739976 a.u.)	0	66	34
MetSN-OH + 4H_2O *II* (-1260.48276 a.u.)	0	62	38

Table 5. Weights ω_i (in %) of the three VB complexes computed at the BH&HLYP level of theory (see scheme 1) for different selected geometries, as inferred from equations 1-3, using the QTAIM spin densities.

From these values, and the previous analysis, the nature of the interactions in the different complexes can readily be inferred. Let's start with geometry I. With a PCM model only as the solvent (first line in Table 5), the VB structure 2 comes out as the major one, with structures 1 and 3 as minor but not negligible. The electronic structures change substantially when the four water molecules are added (second line in Table 5), with a marked increase of the weight of the VB structure 1, from 24% to 45%, and a collapse from 11% to 1% of the weight VB structure 3, which now becomes totally negligible. All in all, almost equal VB weights for 1 and 2 are obtained for geometry I in the presence of four water molecules, which enables us to unambiguously conclude to the existence of a (2c-3e) bond between S and OH in this geometry. This is unprecedented, because complete (2c-3e) bonds in overall neutral compounds in general, and in the S-OH case in particular, are very rare, the difference in charge between the two resonance contributors (1 and 2 here) usually leads to a dominant neutral SOH Valence Bond structure. Quite different is the case of ***II*** (third and fourth lines in Table 5). For the latter, the weight of VB structure 1 is zero, which is consistent with the OH being remote from the sulfur atom. The weights of VB structures 2 and 3 do not change much with the introduction of the four water molecules, and come out as rather balanced, indicative of a (2c,3e) bond between the sulfur and nitrogen atoms within the cationic $MetSN^+$ fragment, in electrostatic interaction with an OH^-.

The oxidation mechanism of sulfur containing molecules has led to hot debates. Two dissociation channels are typically invoked, the "homolytic" pathway with a dissociation to ·OH and neutral fragment, meaning that no oxidation took place, and the "heterolytic" pathway with dissociation to $OH^-$and a cationic counterpart. The "homolytic" channel is theoretically the most preferred one, because the separate neutral products are thermodynamically more stable, even in water environment. However, we have found here the electronic structure of complex ***I*** contains a substantial amount of the VB structure 2, corresponding to a $MetSN^+$ cation in interaction with a OH^-; and that the complex almost isoenergetic to complex ***I*** in presence of explicit water molecules, fully corresponds to an interaction between $MetSN^+$ and OH^- (mixing of VB structures 2 and 3). Therefore, in the case of a diabatic dissociation process, the heterolytic pathway appears as a fully plausible one for MetSN–OH in agreement with the wealth of experimental data (see introduction).

To conclude, all these first results shown that the formation of complexes ***I, II.*** and ***IV*** represents a key step leading to the heterolytic dissociation of Met-$^{\bullet}$OH in $Met^{\bullet+}$ + $^-$OH (radical cations formations).

Results and discussion on the radical cations $Met^{\bullet\bullet+}$

The radical cation either alone or the cluster radical - water molecules were embedded in a continuum. We have first compared both cases to evaluate the importance of the discrete water molecules, following the same methodology as for the adducts.

$MetSN^{\bullet+}$and **$MetSO^{\bullet+}$+ CPCM.** First, we have performed various scan optimization of d_{SN} and d_{SO} i.e. one of these distances was frozen while the other one was gradually raised, the remaining of structural parameters were fully optimized at each step at the BHHLYP/6-311+g(d,p)+ CPCM level of theory**.** Table 6 gathers obtained structural parameters together with QTAIM analysis for the most stable structures.

	MetSN$^{\bullet+}$	**MetSO$^{\bullet+}$**
E + 878	-0.82585	-0.80412
ΔE	0.0	57.0
d_{SN}	2.49	3.45
d_{SO}	3.34	2.72
$d_{SO(CH3)}$	4.80	4.59
ρ_S ; $\rho_{X=N\ or\ O}$	0.52 0.40	0.84 0.06
Q_S ; $Q_{X=N\ or\ O}$	0.27 -1.06	0.46 -1.22

Table 6. Most stable conformations of the scans SN/SO for **MetSN$^{\bullet+}$** and **MetSO$^{\bullet+}$** structures computed at the BHHYP/6-311+G(d,p) + CPCM level of theory. Electronic energies (E) are given in a.u.. ΔE is the relative energy given in kJ/mol with respect to the structure **MetSN$^{\bullet+}$**. Intramolecular distances S-N and S-O (both O of the carboxylate terminal) are given in Å. QTAIM spin densities ρ_S ; $\rho_{X=N\ or\ O}$ and charges Q_S ; $Q_{X=N\ or\ O}$ for radical cations **MetS$^{\bullet+}$** are given in a.u.

The most stable cation is MetSN$^{\bullet+}$**,** with d_{SN} =2.49 Å, a SN2c 3e bond and a relatively small distance between the sulfur and the oxygen of the carbonyl group d_{SO} (3.34 Å). The equivalent with d_{SO} = 2.7 Å has a much higher energy (more than 50 kJ/mol above that of MetSN$^{\bullet+}$). The spin densities do not in agreement with a SO 2c-3e picture. Indeed, the structure is more consistent with a typical **MetS$^{\bullet+}$**cation in agreement with the strong spin density mainly localized on the sulfur atom (0.84 a.u.).

Met$^{\bullet+}$+4 H_2O + CPCM. Like for adducts, the 4 H_2O mimic the first solvation shell and were selected from their short distances to the polar groups of Met, >COCH3, >CO, -NH and >S. The energy of the cluster Met$^+$+ 4 H_2O was calculated at the BH&HLYP/ 6-311+g(d,p) + CPCM level. The 4 water molecules were connected together by a H-bonds network. In Table 7, are summarized main structural parameters together with QTAIM analysis of optimized conformations of the MetSX$^{\bullet+}$ cations. The optimized conformations are displayed in Figure 4. The found most stable conformer is still **MetSN$^{\bullet+}$,** MetSO$^{\bullet+}$ becoming **MetS$^{\bullet+}$**. Both conformations of the cations are quasi-isoenergetic (only 10 kJ/mol between them).

	MetSN$^{\bullet+}$+4 H_2O	**MetSO$^{\bullet+}$+4 H_2O**
E + 1184	-0.53960	-0.52437
ΔE	0.0	39.9
d_{SN}	**2.50**	4.81
d_{SO}	5.09	**2.39**
$d_{SO(CH3)}$	5.25	4.49
ρ_S ; $\rho_{X=N\ or\ O}$	0.**50** **0.42**	**0.82** 0.12
Q_S ; $Q_{X=N\ or\ O}$	0.23 -1.08	0.45 -1.21

Table 7. Most stable conformations of the scans SN/SO for MetSX$^{\bullet+}$+4 H_2O calculated at the BHHYP/6-311+G(d,p) + CPCM level of theory. Electronic energies (E) are given in a.u.. ΔE is the relative energy with respect to the structure **MetSN$^{\bullet+}$+ 4 H_2O** given in kJ/mol. Intramolecular distances S-N, S-O (both O of the carboxylate terminal) are given in Å. QTAIM spin densities ρ_S ; ρ_X and charges Q_S, Q_X for radical cations **MetS$^{\bullet+}$** are given in a.u..

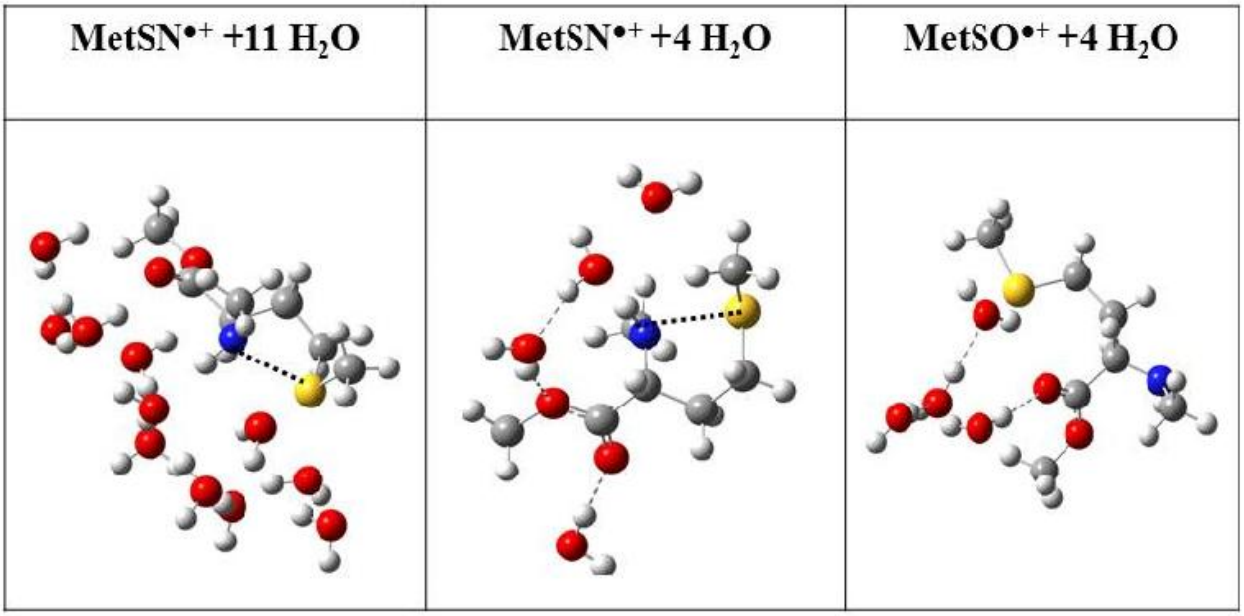

Figure 4. Conformations of the optimized radical cations MetSX+y H_2O (y= 11 or 4). Dotted lines: hydrogen bonds. The S-N bond is underlined by **bold** dotted line.

Since we are dealing with cations, the solvation layer might be more important than for neutral adducts. Therefore we have increased the number of water molecules. We have proceeded in two steps. First, from the results of Molecular Dynamics and scans (not shown), we have selected 15 different conformations of the radical cations from folded **MetSN** and **MetSO** to extended. They were surrounded by different shells of water molecules ($Met^{\bullet+}$ + x H_2O; x=7 or 11). DFT Calculations have been performed at the BHHLYP/6-31g(d) + CPCM level. The changes of energy with respect to the both distances d_{SN} and d_{SO} are displayed in Figure 5 for x = 7 or 11.

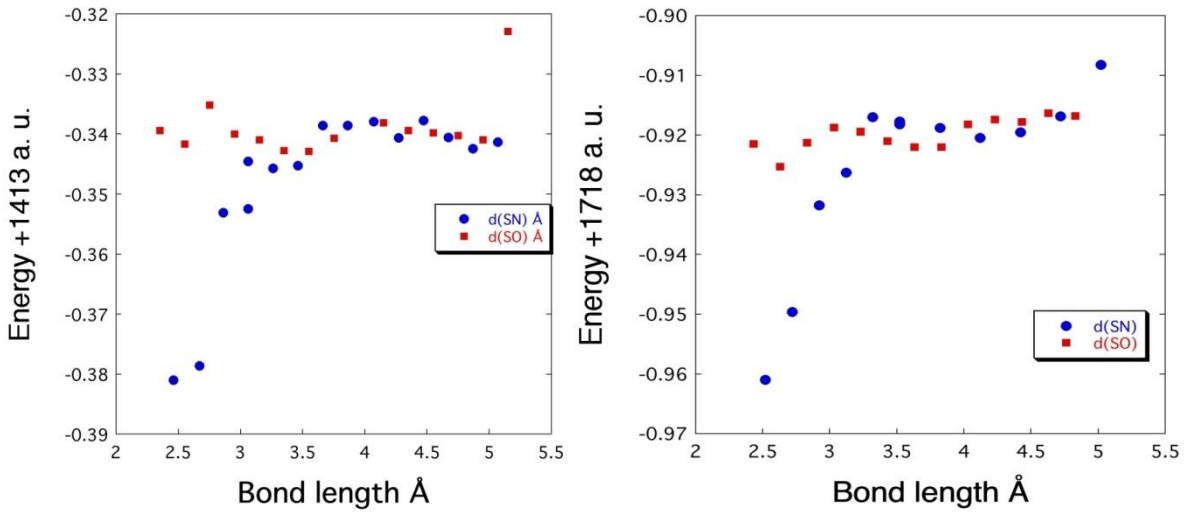

Figure 5. Energy clusters $Met^{\bullet+}$ + x H_2O with x= 7 (left) and x= 11 (right) with respect to both distances d_{SN} (blue dots) and d_{SO} (red dots). Conformations were optimized at the BHHLYP/6-31g(d)+ CPCM level of theory for each distance d_{SX} from a folded conformer (d_{SX} = 2.5Å) to unfolded conformer (d_{SX} = 5.5Å) using a step of 0.25 Å.

These curves are very similar whatever the number of water molecules taken into account. The energy minimum for both curves is for a 2c-3e SN bond of 2.5 Å. Further data have been obtained with a crude analysis of the landscape of the potential electronic energy surface (PES), carried out for the clusters $Met^{\bullet+}$+ 11 H_2O displayed in Figure 6.

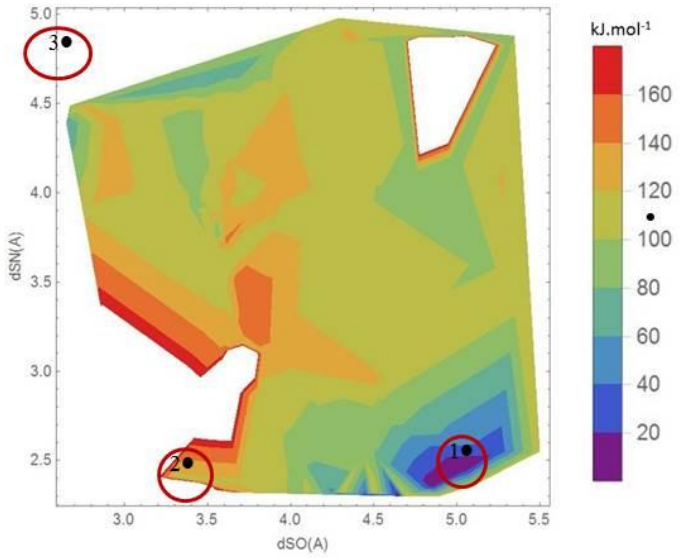

Figure 6. Potential Energy Surface E = f(d_{SN}, d_{SO}) for clusters $Met^{\bullet+}$+ 11H_2O computed at the BHHLYP/6-31g(d)+ CPCM level of theory. Conformations obtained from folded (d_{SX} = 2.5Å) to unfolded ones (d_{SX} = 5.5Å) by steps of 0.25 Å.

Three regions on the PES have been identified (see Figure 6): a small zone (purple to dark blue) corresponds to the most stable conformation. The SN bond is short (*ca.* 2.4 Å) and the SO one is long (*ca.* 5 Å). Interestingly the "point 1", which corresponds to the energetic minimum with only 4 water molecules, is situated in the purple zone.

The second one (green-blue) is divided in several parts, the SN bond of ca. 2.5 Å and the SO bond of ca. 4 to ca. 5.5 Å ; the SN and SO bonds around 4-5 Å; the SO bond smaller (*ca.* 3 Å)and SN around 4.5 Å. The energies have been found around 60 kJ/mol higher than that of the minimum. The "points 2 and 3" fall into these zones of high energy. The third one (green-yellow) is constituted of a large plateau with energies higher than 100 kJ/mol. This plateau is too high to allow transformation between SN and SO.

To conclude, the stable cations display S-N bonds rather than S-O bonds, these latter being much higher in energy. It is worth noting that a very high plateau separates the two different compounds of radical cations which suggests that no reasonable transformation from SO to SN bond is kinetically expected.

Conclusions

The goal of this study was focused on the analysis of the electronic factors governing the first steps of the oxidation, formation of OH- adducts and possibilities of heterolytic ruptures. We compared several methods describing the solvent: CPCM only, molecular mechanics description of water molecules (QM/MM) taken from MD snapshots, CPCM with several water molecules coming also from MD snapshots. We found that a small number of water molecules was sufficient to get a more precise description (4 for neutral species with large basis set; 7-11 for charged species with smaller basis set).

The second problem we had to face was the endgroups. We chose to add methyl groups to get rid of the electrostatic interactions of the zwitterion. In the literature, the problem of end groups of Met was solved differently: by letting crude charged groups [22]; more recently by putting peptidic bonds [20].

We performed some calculations for the complex ***III*** where the NH_2CH_3 endgroup was replaced by either $–NH_3^+$ or amide. When the $–NH_3^+$ endgroup was used, the trends were identical to those where $–NH_2CH_3$ endgroup was used ,.i.e. H transfer between OH and NH_3. In contrast, there is reorganization of Met and formation of a (2c-3 e) SN bond (Table 2) if the amide endgroup is used.

Major new insights were obtained:

1) Several positions of OH radical vs. Met were found concomitant with the different positions of water molecules. The probability of OH radical to attack any atom is well known in pulse radiolysis although the rate constants are different. For instance OH could be close to –NH, far from S etc..
2) When OH was close to N and far from S (complex ***III***) a H transfer from the amino group to $^{\bullet}OH$ took place leading to the formation of water molecule and N-centered radical. This radical was the most stable one. This H transfer could occur directly or through a network of hydrogen bonds linking water molecules. When the amine was charged ($–NH_3^+$) or replaced by an amide, the same result was obtained. It was independent of the method of solvent description. The N-centered radical did not undergo folding, excluding the formation of a 2c-3e S-N.
3) The first solvation shell has a great importance for the stabilization energies. With discrete water molecules ***I*** and ***II*** have very close energies while they differed by *ca*. 80 kJ/mol using only a CPCM.

4) VB analysis allowed obtaining probability of heterolytic rupture, which was modified by the presence of water molecules. It is notably important but not equal to 100% hence a mixture of cations and OH adducts should be present in solutions. The heterolytic rupture is specially probable with MetS-$^{\bullet}$OH ***I***, like in DMS adducts. In ***II***, the 2c-3e S-N bond is prone to this heterolytic rupture because of stabilization by the presence of the 4 water molecules.
5) After having explored a large zone of geometries of the cation going from folded to extended, a small stability zone was found corresponding to 2c 3e SN bonded radical, consistently with our previous calculations [10,13]. Conversely, our former calculations [13,14] on peptides (MetGly, GlyMet and MetMet) led to several stable cyclic conformations (from 5 to 9 members) with MetSN$^{\bullet+}$ as well asMetSO$^{\bullet+}$ bonds.

The future of these free radical is to give birth to the final products that have been detected [15-17]. One should keep in mind that subsequent reactions take place in solution (e.g. disproportionation, hydration, decarboxylation…). For instance a sulfoxide can be created either from an OH adduct or from disproportionation and hydration. The CC double bond necessitates electron transfer from sulfur to adjacent carbon. Decarboxylation could come from electron transfer between N centered radical and carboxylate group.

Compliance with ethical standards

Conflict of interest: The authors declare that they have no competing interests.

References

1. Asmus KD, Janata E (1982). In:Baxendale JH, Busi F, Reidel D (ed) The Study of Fast Processes and Transient Species by Electron Pulse Radiolysis Publishing Company Dordrecht, pp 115-128
2. Asmus KD (2001).In:Jonah CD, Rao BMSR (ed) Radiation Chemsitry: present status and future trends Elsevier, New York, pp 341-393
3. Bobrowski K, Hug GL, Pogocki D, Marciniak B, Schoneich C (2007). J Phys Chem B111: 9608
4. Bobrowski K, Houée Levin C, Marciniak B (2008).Chimia 62:728
5. Ignasiak M, Marciniak B, Houée Levin C (2014). Isr J Chem 54:225
6. Ignasiak M, Scuderi D, de Oliveira P, Pedzinski T, Rayah Y, Houée Levin C(2011).Chem Phys Letters 502: 29
7. Ignasiak M, de Oliveira P, Houée Levin C, Scuderi D (2013). Chem Phys Lett 590:35
8. Ignasiak M, Pedzinski T, Rusconi F, Filipiak P, Bobrowski K, Houée-Levin C, Marciniak B (2014). J Phys Chem B 118:8549
9. Buxton G, Greenstock CL, Helman WP, Ross AB (1988). J Phys Chem 17:513

10. Archirel P, Bergès J, Houée-Levin C (2016). J Phys Chem B 120:9875
11. Bergès J, de Oliveira P, Fourré I, Houée-Levin C (2012). J Phys Chem B 116:9352
12. Bergès J, Kamar A, de Oliveira P, Pilmé J, Luppi E, Houée-Levin C (2015). J Phys Chem B 119: 6885
13. Fourré I, Bergès J, Houée-Levin C (2010). J Phys Chem A 114:7359
14. Fourré I, Bergès J, Braïda B, Houée Levin C (2008). Chem Phys Lett 467:164
15. Scuderi D, Bergès J, de Oliveira P, Houée-Levin C, (2016) Radiat Phys Chem 128:103
16. Scuderi D, Ignasiak M, Serfaty X, de Oliveira P, Houée Levin C (2015). PhysChem Chem Phys 17: 25998
17. Perdivara I, Deterding LJ, Przybylski M, Tomer KB (2010). J Amer Soc Mass Spect 21:1114
18. Pilmé J, Luppi E, Bergès J, Houée-Levin C, de la Lande A (2014). J Mol Model 20: 2368
19. Xipsiti C, Nicolaides AV (2013). Comput Theor Chem 1009:24
20. Uranga J, Mujika JI, Matxain JM (2015). J Phys Chem B 119:15430
21. Chu JW, Brooks BR, Trout BLJ (2004). J Amer Chem Soc 126:16601
22. Marino T,Soriano-Correa C, Russo N (2012). J Phys Chem B 116:5349
23. Domin D, Braïda B, Bergès J (2017). J Phys Chem B 121:9321
24. Shaik S, Braïda B, Wu W, Hiberty PC (2016). In:Mingos DMP (ed) Chemical Bond II: 100 Years Old and Getting Stronger, Springer: Switzerland 170, pp 169
25. Danovich D, Foroutan-Nejad C, Hiberty PC, Shaik S (2018). J Phys Chem A 122:1873
26. Jorgensen WL, Chandrasekhar J, Madura JD (1983). J Chem Phys 79:926
27. MacKerell Jr AD, Bashford D, Bellott M, et al (1998). J Phys Chem B 102:3586
28. Frisch MJ, Trucks GW, Schlegel HB, Scuseria GE, Robb MA, Cheeseman JR, Scalmani G, Barone V, Mennucci B, Petersson GA, Nakatsuji H, Caricato M, Li X, Hratchian HP, IzmaylovAF, Bloino J, Zheng G, Sonnenberg JL, Hada M, Ehara M,Toyota K, Fukuda R, Hasegawa J, Ishida M, Nakajima T, HondaY, Kitao O, Nakai H, Vreven T, Montgomery JA Jr, Peralta JE,Ogliaro F, Bearpark M, Heyd JJ, Brothers E, Kudin KN, Staroverov VN, Kobayashi R, Normand J, Raghavachari K,Rendell A, Burant JC, Iyengar SS, Tomasi J, Cossi M, Rega N,Millam JM, Klene M, Knox JE, Cross JB, Bakken V, Adamo C,Jaramillo J, Gomperts R, Stratmann RE, Yazyev O, Austin AJ,Cammi R, Pomelli C, Ochterski JW, Martin RL, Morokuma K, Zakrzewski VG, Voth GA, Salvador P, Dannenberg JJ, Dapprich S, Daniels AD, Farkas Ö, Foresman JB, Ortiz JV, Cioslowski J,Fox (2009) Gaussian 09. vol D.01. Wallingford CT
29. Bader RFW (1991).Chem Rev 91:893
30. Bader RFW, Stephens ME (1975). J Amer Chem Soc 97:7391
31. Fradera X, Austen MA, Bader RFW (1998). J Phys Chem A 103:304
32. Braïda B, Hiberty PC, Savin A(1998). J Phys Chem A 102:7872
33. Braïda B, Hiberty PC (2000). J Phys Chem A 104:4618
34. Braïda B, Lauvergnat D, Hiberty PC (2001). J Chem Phys 115:90